Uniformity of Illumination of Spherical Laser Fusion Targets

J.E. Howard

August 20, 1976

UWFDM-172

FUSION TECHNOLOGY INSTITUTE

UNIVERSITY OF WISCONSIN

MADISON WISCONSIN

Uniformity of Illumination of Spherical Laser Fusion Targets

J.E. Howard

Fusion Technology Institute
University of Wisconsin
1500 Engineering Drive
Madison, WI 53706

http://fti.neep.wisc.edu

August 20, 1976

UWFDM-172

"LEGAL NOTICE"

"This work was prepared by the University of Wisconsin as an account of work sponsored by the Electric Power Research Institute, Inc. ("EPRI"). Neither EPRI, members of EPRI, the University of Wisconsin, nor any person acting on behalf of either:

"a. Makes any warranty or representation, express or implied, with respect to the accuracy, completeness, or usefulness of the information contained in this report, or that the use of any information, apparatus, method, or process disclosed in this report may not infringe privately owned rights; or

"b. Assumes any liabilities with respect to the use of, or for damages resulting from the use of, any information, apparatus, method or process disclosed in this report."

Uniformity of Illumination of Spherical Laser Fusion Targets

James E. Howard
University of Wisconsin, Nuclear Engineering Department, Madison, Wis. 53706

Uniformity of illumination of spherical laser fusion targets is calculated for 8, 12 and 20 beams arranged according to the symmetry of the Platonic solids. Uniformity was optimized by varying the f/no. of ideal aberration-free lenses, amount of beam overlap, and the shape of the spatial beam profile. The numerical results show 20 beam illumination to be slightly better than 12 beam illumination, with 8 beams running a poor third. Refractive energy losses due to nonorthogonal illumination and the implications for the design of a practical laser fusion reactor are discussed.

1. Introduction

In the laser fusion process, a small sphere of deuterium-tritium fuel is heated and compressed to thermonuclear burn conditions by intense laser beams.[1] The thermonuclear yield (and therefore the plant efficiency) depends sensitively on the implosion symmetry, which, at least in its early phase, demands very uniform irradiance over the pellet surface.[2] Many schemes have been proposed for illuminating fusion targets, ranging from one[3] to several-hundred beams[4] in various combinations of lenses[5] and mirrors.[6] In this paper we describe the calculation of irradiance on a spherical surface due to N overlapping beams, with N = 4, 6, 8, 12 or 20, corresponding to the symmetry of the five Platonic solids. Provision is currently made for the following spatial beam profiles; flat, Gaussian, and "supergaussian." Ideal lenses were employed as focusing elements, although aplanatic lenses could equally well have been used.

Basically, our task is to provide a specified uniformity of illumination over the entire pellet surface, keeping the rays as normal to the surface as possible. The required degree of uniformity is determined chiefly by its effect on growth of the Rayleigh-Taylor instability,[2] while the angles of incidence must be held down in order to maximize inverse bremsstrahlung absorption, and minimize refraction in the blowoff layer.[7]

To control pellet irradiance, we have at our disposal four independent quantities; N, the number of beams, δ, the shift of the beam focus relative to the pellet center, F, the f/no. of the focused beam, and the beam profile $I_o(r)$, where r is the beam radius on the last optical element (lens or mirror). The beam profile may depend on 2-3 parameters, so it would seem we have a formidable parameter space to deal with. In practice, however, only a few values of N are considered, F then being determined by the maximum solid angle allotted to optics. Of course, the optics must be sufficiently distant from the target so that the beam aperture is adequate to handle the energy and power per beam as well as the radiation and debris from the target. The total aperture area is determined in practice by material damage constraints on the beam energy, rather than self-focusing constraints on the beam power.[8]

A more complete treatment of the uniformity problem would entail following the energy deposition in the early phases of the corona expansion, taking into account refraction and lessened energy absorption near the beam edges where the angles of incidence are largest.

2. The Platonic Solids

A sphere may be partitioned into N equal-solid-angle wedges by means of the five Platonic solids, illustrated in Fig. 1. A sphere may also be divided into two equal solid angle portions by

means of a plane cut through its center.* Other partitions are possible. For example, beams placed at each of the 12 vertices of an icosahedron allows symmetric placement of 32 beams. The Ω-10 facility at Rochester[9] is designed for 24 beams.

Each Platonic solid being made up of N regular polygonal faces, it is customary to classify them according to the number of sides (p) of the polygons and the number of adjacent faces (q) at a vertex. Given the number of faces N_S, it is easy to show that the number of edges and vertices are given by

$$N_E = 1/2\ p\ N_S \tag{1}$$

$$N_V = \frac{p}{q} N_S\ . \tag{2}$$

These numbers are related by Euler's formula,[10]

$$N_V + N_S - N_E = 2\ . \tag{3}$$

We shall also need the dihedral angle α and the wedge angle β, as depicted in Fig. 2.

---

* I have recently learned of the existence of a sixth degenerate Platonic solid, the "dihedron," a double plane polygon enclosing no volume.[11]

$$\sin\frac{\alpha}{2} = \cos\frac{\beta}{2} = \frac{\cos(\pi/q)}{\sin(\pi/p)} \tag{4}$$

$$\beta = \pi - \alpha \ .$$

Table 1 lists these parameters for all of the Platonic solids. Since laser beams are circular rather than prismatic, it is necessary to overlap them in order to cover the entire pellet surface. Uniform illumination may be obtained by simultaneously varying the degree of overlap and contouring the beam profile. In Section 4 we shall use Table 1 to determine the coordinates of all beams relative to a common origin and combine intensities in the overlap regions.

3. Intensity Profiles

Assuming ideal lenses, each beam contributes an irradiance[6]

$$I(\theta) = I_o(r)\left(\frac{f}{R_T}\right)^2 \frac{1 + \delta\cos\theta}{(\cos\theta + \delta)^3} \quad W/cm^2 \ , \tag{5}$$

where $I_o(r)$ is the flux incident on the lens, r is the beam radius, R_T the target radius, f is the focal length, and

$$\delta = \Delta x/R_T \tag{6}$$

measures the focal shift relative to the target center (Fig. 3).

The angle of incidence Ψ is given in terms of the beam half-angle ξ and δ by

$$\sin\Psi = \delta\sin\xi \ . \tag{7}$$

The beam half angle is related to the f/no. by

$$\cot\xi = 2F \ . \tag{8}$$

Thus, the maximum angle of incidence is given by

$$\sin\Psi_{max} = \frac{\delta}{\sqrt{1+4F^2}} \quad . \tag{9}$$

It is essential that Ψ_{max} be made as small as possible in order to minimize laser energy lost through refraction in the pellet corona.[7]

Now when we come to optimize pellet illumination uniformity, the outcome will be a certain spot size as measured by the pellet central angle θ_{max}. From Fig. 3, the corresponding focal shift is given by

$$\delta = 2F \sin\theta_{max} - \cos\theta_{max} \quad . \tag{10}$$

So the price we pay for uniformity is given by combining eqs. (9) and (10):

$$\sin\Psi_{max} = \frac{2F \sin\theta_{max} - \cos\theta_{max}}{\sqrt{1+4F^2}} \quad , \tag{11}$$

which is just another way of writing

$$\Psi_{max} = \theta_{max} - \xi \quad . \tag{12}$$

Equation (12) shows that if θ_{max} is large, then ξ must also be large in order to keep Ψ_{max} small. From eq. (8), we see that large ξ naturally translates into small f/no.

Unlike a research facility such as SHIVA,[5] the beam transport system in a laser fusion reactor (LFR) can only take up a small fraction of the

solid angle subtended to the target. Whereas SHIVA has about 50% of its solid angle devoted to beams, an LFR is limited to about 10% for economic reasons. Each beam occupies a solid angle

$$\Delta\Omega = 2\pi(1 - \cos\xi) , \tag{13}$$

so that the total fractional solid angle taken up by N beams is

$$\gamma = \frac{N\Delta\Omega}{4\pi} = \frac{N}{2}\left[1 - \frac{2F}{\sqrt{1+4F^2}}\right] . \tag{14}$$

Solving for F, we find, for $\gamma << 1$,

$$F_{min} = \frac{\frac{1}{2}\left(1 - \frac{2\gamma}{N}\right)}{\sqrt{1 - \left(1 - \frac{2\gamma}{N}\right)^2}} \simeq \frac{1}{4}\sqrt{\frac{N}{\gamma}} . \tag{15}$$

This is the minimum f/no. required to occupy less than a specified solid angle fraction. Table 2 lists F_{min} for $\gamma = 0.1$ and 0.2. For $\gamma << 1$, the maximum angle of incidence is

$$\Psi_{max} \simeq \theta_{max} - 2\sqrt{\frac{\gamma}{N}} . \tag{16}$$

The small-angle results, eqs. (15) and (16) are not substantially changed by the use of aplanatic lenses, for which

$$\csc\xi = 2F \tag{17}$$

replaces eq. (8). In general, the angles of incidence decrease as more beams are added, assuming equal target coverage and fixed γ. However, it will be seen that in the important cases N = 12 and 20, the optimal values of θ_{max} are nearly equal, independent of γ, so that the angles of incidence are actually somewhat larger for 20 beams.

We are now in a position to design a pellet illumination scheme, proceeding as follows:

1. Choose a definite fractional solid angle γ, say 10%.
2. Choose the number of beams, say N = 12 or 20.
3. This fixes the minimum f/no. by eq. (15).
4. Next choose a beam profile, say Gaussian.
5. Vary δ until the uniformity exceeds the desired value, say 90%. This number directly affects the Rayleigh-Taylor growth rate.[2]
6. The optimum δ and F determines θ_{max} from eq. (10):

$$\sin\theta_{max} = \frac{2F\delta + \sqrt{1 + 4F^2 - \delta^2}}{1 + 4F^2} \quad . \tag{18}$$

7. Eq. (11) or (16) determines Ψ_{max}.
8. Ψ_{max} determines the amount of laser energy lost due to refraction.
9. If Ψ_{max} is too large, one has two main options:
   (a) relax the uniformity requirement (5)
   (b) relax the solid angle requirement (1).

4. Calculating Beam Overlap

Before carrying out the above optimization procedure, we have to learn how to calculate the intensity due to a number of overlapping spots. We shall examine here only the cases N = 8, 12, and 20; octahedral, dodecahedral and icosahedral. High uniformity is not possible using 4 or 6 beams, so these configurations will not be considered further in this paper.

First of all, by symmetry we need only look at a single pie slice-shaped region, as depicted in Fig. 4 for the icosahedron (only 3 nearest neighbor spots are shown). In this case, only spots 0 and A need be included. In general, however, several spots (located at points Q_k) may contribute to the intensity at point P according to eq. (5) with θ_{PQ_k} given by

$$\cos\theta_{PQ_k} = \cos\theta\,\cos\theta_k + \sin\theta\,\sin\theta_k\,\cos(\phi - \phi_k) \quad (19)$$

as shown in Fig. 4.

The coordinates of the neighboring beams are conveniently found by means of the Schlegel diagram.[10] This is simply a two-dimensional projection of the polyhedron gotten by bringing one face up to the eye.

4.1 Octahedron

We wish to locate points Q_k, k = 1,6 w. r. t. point 0, using the Schlegel diagram depicted in Fig. 5. The 8th (opposite) point will be ignored. The fundamental pie slice has its 60^o wedge at point 0, with one side along the arc $0Q_k$. From Table 1, the angular side $\beta = 70.53^o$. We want to solve the spherical triangle $0Q_1Q_4$ for the angular side θ_4. By the cosine law, $\cos\theta_4 = -1/3$ so that $\theta_4 = \pi - \beta$. Thus,

$$\begin{array}{ll} \phi_1 = 0 & \theta_1 = \beta = 70.53^o \\ \phi_2 = 120^o & \theta_2 = \beta \\ \phi_3 = 240^o & \theta_3 = \beta \\ \phi_4 = 60^o & \theta_4 = 180^o - \beta = 109.47^o \end{array}$$

$$\phi_5 = 180^o \qquad \theta_5 = \theta_4$$
$$\phi_6 = 300^o \qquad \theta_6 = \theta_4$$

4.2 Dodecahedron

Figure 6 shows the Schlegel diagram; again the opposite 12th face is ignored. In this case, the fundamental pie slice subtends a 36^o angle. From Table 1, $\beta = 63.43^o$. Solving the spherical triangle OQ_1Q_6 we find $\theta_6 = \pi - \beta$. Thus,

$$\phi_1 = 0 \qquad \theta_1 = \beta = 63.43^o$$
$$\phi_2 = 72^o \qquad \theta_2 = \beta$$
$$\phi_3 = 144^o \qquad \theta_3 = \beta$$
$$\phi_4 = 216^o \qquad \theta_4 = \beta$$
$$\phi_5 = 288^o \qquad \theta_5 = \beta$$
$$\phi_6 = 36^o \qquad \theta_6 = \pi - \beta = 116.57^o$$
$$\phi_7 = 108^o \qquad \theta_7 = \theta_6$$
$$\phi_8 = 180^o \qquad \theta_8 = \theta_6$$
$$\phi_9 = 252^o \qquad \theta_9 = \theta_6$$
$$\phi_{10} = 324^o \qquad \theta_{10} = \theta_6$$

4.3 Icosahedron

Figure 7 depicts the Schlegel diagram; only the inner hexagonal portion is needed for $\theta_{max} \leq 72^o$. Solving the spherical triangle OQ_1Q_4 gives

$$\cos\theta_4 = 1 - \frac{3}{2}\sin^2\beta ,$$

where $\beta = 41.82^o$. Thus, $\theta_4 = 70.53^o$, which is just the octahedron wedge angle! In this case, we must also calculate the angle ϕ_4. By the sine law,

$$\sin\phi_4 = \frac{\sin\beta \sin 60^o}{\sin\theta_4} = \frac{\sqrt{3}}{2\sqrt{2}} ,$$

so that $\phi_4 = 37.76^o$. The coordinates of points 10-18 may be found by solving spherical triangles 0-4-11 and 0-1-18. The results are

$$\phi_1 = 0 \qquad \theta_1 = \beta = 41.82^o$$
$$\phi_2 = 120^o \qquad \theta_2 = \beta$$
$$\phi_3 = 240^o \qquad \theta_3 = \beta$$
$$\phi_4 = 37.76^o \qquad \theta_4 = 70.53^o$$
$$\phi_5 = 120^o - \phi_4 \qquad \theta_5 = \theta_4$$
$$\phi_6 = 120^o + \phi_4 \qquad \theta_6 = \theta_4$$
$$\phi_7 = 240^o - \phi_4 \qquad \theta_7 = \theta_4$$
$$\phi_8 = 240^o + \phi_4 \qquad \theta_8 = \theta_4$$
$$\phi_9 = 360^o - \phi_4 \qquad \theta_9 = \theta_4$$
$$\phi_{10} = 60^o - \phi_4 \qquad \theta_{10} = 180^o - \theta_4$$
$$\phi_{11} = 60^o \qquad \theta_{11} = 180^o - \beta$$
$$\phi_{12} = 60^o + \phi_4 \qquad \theta_{12} = 180^o - \theta_4$$
$$\phi_{13} = 180^o - \phi_4 \qquad \theta_{13} = 180^o - \theta_4$$
$$\phi_{14} = 180^o \qquad \theta_{14} = 180^o - \beta$$
$$\phi_{15} = 180^o + \phi_4 \qquad \theta_{15} = 180^o - \theta_4$$
$$\phi_{16} = 300^o - \phi_4 \qquad \theta_{16} = 180^o - \theta_4$$
$$\phi_{17} = 300^o \qquad \theta_{17} = 180^o - \beta$$
$$\phi_{18} = 300^o + \phi_4 \qquad \theta_{18} = 180^o - \theta_4$$

4.4 Minimum Value of θ_{max} for Total Coverage

Having located the positions of all beams, we can now calculate the irradiance on a sphere with an arbitrary amount of overlap. From Fig. 4, we see that the condition for the spots to just touch is

$$\theta_{max} = \beta/2 \ . \qquad (20)$$

Thus, a focal shift of at least

$$\delta_{min} = 2F \sin\beta/2 - \cos\beta/2 \qquad (21)$$

is needed in order to achieve uniform irradiance. When the beams overlap sufficiently, there will be no unilluminated areas on the pellet. To calculate θ_{max} for 100% coverage, we must look at each case individually.

Octahedron

Figure 8 depicts the four nearest neighbor beams. In order to cover the small rectangular area in the center, we solve the triangle O1P. The law of sines gives

$$\sin\theta_m^* = \sin 60^o \sin\beta = \left(\frac{1}{2}\sqrt{3}\right)\left(\frac{2}{3}\sqrt{2}\right) = \sqrt{2/3} \quad , \qquad (22)$$

or

$$\theta_m^* = \tan^{-1}\sqrt{2} = 54.74^o \quad .$$

Dodecahedron

Figure 9 shows the three nearest neighbor spots. To wipe out the triangular hole in the center, we solve the spherical triangle OP2 and find

$$\sin\theta_m^* = \frac{\sin 36^o}{\sin 60^o}\sin\beta = 0.607 \quad , \qquad (23)$$

so that

$$\theta_m^* = 37.38^o \quad .$$

Icosahedron

Figure 10 shows the five nearest spots. Solving the spherical triangle OP2 gives

$$\sin\theta_m^* = \frac{\sin 60^o \sin\beta}{\sin 72^o} = 0.607 \ . \qquad (24)$$

Thus, $\theta^*_{max} = 37.38^o$, the same value as for the 12 beam case!

5. Numerical Results

A computer program, PLATO, has been written to calculate irradiance profiles over the fundamental region for each of the configurations described in Section 4. We first examine SHIVA-type designs,[5] using 8, 12 and 20 f/1.5 lenses. Next, reactor-type configurations are considered, with optics limited to 10 or 20% of the total solid angle seen by the target. (Of course, SHIVA was never intended to resemble a reactor; its 20 beams take up 51% of the total solid angle.) In all cases, greater than 90% uniformity is realizable using 12 or 20 beams, with 8 beams running a poor third. However, good uniformity for the high f/nos. typical of reactor configurations can only be achieved at the expense of large angles of incidence and consequent loss of laser energy by refraction in the plasma corona.[7]

5.1 Optimization

In following the optimization procedure outlined in Section 3, we first fix F = 1.5 and treat the cases N = 8, 12 and 20 separately. Spatial beam profiles were chosen from the two-parameter family of "supergaussian" forms,

$$I_o(r) = \bar{e}^{(r/a)^p}, \tag{25}$$

with p = 2, 3, 4 and 5. The parameter a is related to the half width at half-maximum by

$$x_{1/2} = a(\ell n 2)^{1/p} . \tag{26}$$

The irradiance, including overlap from all beams, is then computed on a mesh (θ,ϕ) over the fundamental region, for a number of values of θ_{max}. Extracting the maximum and minimum, we calculate the uniformity

$$\eta = 1 - (I_{max} - I_{min})/(I_{max} + I_{min}) . \tag{27}$$

To interpret this criterion, consider a sinusoidal ripple of amplitude A superimposed on a DC signal of magnitude B. It is natural to express the deviation from constancy or A/B and the uniformity as 1-A/B. In contrast, the Livermore studies[5] use $\eta_L = I_{min}/I_{max} \leq \eta$. Note that both η and η_L vary between 0 and 1.

Figures 11-13 show η as a function of θ_{max} for Gaussian profiles (p = 2), having width parameters a = 0.5, 1.0 and 0.70 (Fig. 14). Clearly, best uniformity is obtained for a = 0.7, the optimal value for this profile. Notice the great improvement in going from 8 to 12 beams, and the smaller but non-negligible improvement in going from 12 to 20 beams. Although the curves

sometimes cross, the 12 and 20 beam cases always seem to improve (or worsen) together. Also note that $\eta = 0$ at $\theta_{max} = 54.7^{o}$ for 8 beams and at $\theta_{max} = 37.4^{o}$ for 12 or 20 beams, as predicted in section 4. As we shall see, a practical illumination system requires $\theta_{max} \lesssim 50^{o}$ in order to keep the angles of incidence reasonably small.

Figure 15 shows optimum uniformity curves for the cubic exponential profile ($p = 3$, Fig. 16). Again all three configurations are optimized together with $a = 0.70$. In this case better than 95% uniformity is obtained for 20 beams and over 93% using 12 beams, considerably better than that found using the Gaussian profile. Only slight improvement was realized by varying p near $p = 3$, while the results for $p = 4$ and 5 were much worse.

The remarkable closeness of the uniformity curves for 12 and 20 beams up to $\theta_{max} \simeq 50^{o}$ suggests little advantage in choosing 20 beams rather than 12. However, the 12 beam curve is rather sharply peaked and might therefore be vulnerable to positioning errors. To investigate this question, let us calculate the change in the focal shift corresponding to a variation in θ_{max} of 2.5^{o}, roughly the half-width of the peak in the 12 beam curve in Fig. 15. From eq. (10) we have

$$\delta(\Delta x) = (2F\cos\theta_{max} + \sin\theta_{max})\, R_T\, \delta\theta_{max}\,, \tag{28}$$

which gives, for $F = 1.5$ and $\theta_{max} = 50^o$,

$$\delta(\Delta x) = 0.047\, R_T\, \delta\theta_{max}\,. \tag{29}$$

Setting $\delta\theta_{max} = 2.5^o$, we get $\delta(\Delta x) \simeq 12$ μm for $R_T = 100$ μm and $\delta(\Delta x) \simeq 120$ μm for $R_T = 1000$ μm.

While laser beams are routinely focused on target to within 5 μm in current laser fusion experiments,[5] maintaining optical alignment of many beams in a reactor environment at a repetition rate of 10-20 Hz is quite another matter. By the time each beam makes several reflections as it wends its way from laser to target, the accumulated jitter could be expected to exceed tens of microns. Thus, it seems reasonable to expect positioning to within 100 μm and thereby to control θ_{max} to within 2.5^o on reactor-size pellets. Smaller pellets can be uniformly illuminated with 12 beams only if sufficient time is available between shots to maintain alignment.

As we have seen, good uniformity also depends critically on the choice of spatial beam profile. Beam tailoring may be effected by soft apertures and Pockels cells.[13] While spatial filters[14] effectively eliminate fine structure, they are unable to remove gross beam inhomogeneities. It is therefore futile to

attempt fine beam tailoring unless the laser train produces a reasonably smooth beam to begin with. The sharp edge on the ideal optimal profile depicted in Fig. 16 may also produce undesirable distortions of the focal region through self-focusing.[15] For this reason (among others) mirrors, rather than lenses, should be used as focusing elements.

A quantity relevant to system efficiency is the fill factor

$$ff = \frac{1}{\pi R_L^2} \int_0^{R_L} I_o(r)\, 2\pi r dr \ , \qquad (30)$$

which measures how well the beam fills the aperture. Table 3 lists fill factors for a number of supergaussian profiles. Note that for a Gaussian,

$$ff = a^2 \left(1 - e^{-1/a^2}\right) . \qquad (31)$$

Now we see that there is something special about the optimal case a = 0.70; it is practically a stationary point for the variation of ff with index p. There is less than a 2% change in ff as p varies from 2 to 5. Table 3 also illustrates the fact that considerable laser energy can be wasted in beam-tailoring.

The 90% uniformity level required to prevent rapid growth of the Rayleigh-Taylor instability is based on analytic studies[2] and numerical simulation.[5] No direct physical measurement has yet been made of this effect. However, recent studies[7]

show that the growth rate may be greatly reduced by controlling the radial density profile in the pellet. Thus, the 90% figure cited should be regarded as tentative, awaiting experimental confirmation.

All of the uniformity curves in Figs. 13 and 14 exceed 95% as θ_{max} approaches 90^{o}. The catch is that the angles of incidence increase with θ_{max} to the point where refractive loss of laser energy becomes prohibitively large. This is illustrated in Fig. 17, which shows Ψ_{max} as a function of θ_{max} for various f/nos. For example, using f/1.5 lenses, the smallest possible value of Ψ_{max} is 18^{o} for 12 or 20 beams. Based on the present studies and those at Livermore, 90% uniformity may be obtained around $\theta_{max} = 50^{o}$ at the least, for which Fig. 17 gives $\Psi_{max} = 32^{o}$. The reflectivity of the pellet corona is approximately $\exp(-2p\cos^{3}\Psi)$, where p is the optical thickness, indicating large refractive losses as $\Psi \to 90^{o}$. However, a detailed calculation,[7] averaging over the optimal beam profile shows only a few percent net energy loss due to oblique incidence when $\theta_{max} = 50^{o}$. Thus, uniform illumination of over 90% can be realized without excessive refractive energy loss.

Another reason for preferring smaller angles of incidence is to maximize resonance absorption.[16] In this process, the p-polarized component of the electric field is strongly absorbed in a range of incident angles depending on the density scale height in the

pellet corona. While the optimal angle of incidence varies from case to case, it is always less than 10^{o}, so that the average angles of incidence ($\Psi \simeq \frac{2}{3}\Psi_{max}$) cited above are too large for effective resonance absorption. However, other effects, such as expansion of the critical surface[7] and self-steepening[17] of the plasma density profile, can improve the match of incident angle to resonance angle. Detailed discussion of these effects is beyond the scope of this paper.

5.2 Solid Angle-Limited Designs

Next we turn to the reactor-type cases where the f/nos. are limited by the fractional solid angle allotted to optics, as listed in Table 2. As before, we consider 8, 12 and 20 beams, but use only the optimal cubic exponential beam profile, with a = 0.70. Figures 18 and 19 show the resulting uniformities for $\gamma = \Delta\Omega/4\pi$ = 0.1 and 0.2. Again the 8 beam configuration runs a poor third. What is perhaps surprising is that the curves are almost identical for N = 20, with only a few percent difference in the N = 12 curves. However, due to the larger f/nos., the angles of incidence are somewhat larger in the γ = 0.1 cases (Fig. 17). For example, for 20 beams at $\theta_{max} = 50^{o}$, $\Psi_{max} = 38.5^{o}$ and 42^{o}, for γ = 0.2 and 0.1, resp. For N = 12, $\Psi_{max} = 36^{o}$ and 39.5^{o}. That is, decreasing γ by a factor of two only increases Ψ_{max} by 10%, a very favorable trade-off indeed!

6. Discussion

We have described the calculation of illumination uniformity on spherical targets for 8, 12 and 20 overlapping beams arranged according to the symmetry of the Platonic solids, using ideal thin lenses as the final optical elements. Due to the extreme symmetry of these configurations, only a small triangular region had to be examined. Other, less symmetrical, illumination schemes would require looking at a larger portion of the sphere and therefore entail more programming. On the other hand, it would be easy to modify PLATO to employ aplanatic lenses, or parabolic mirrors. Further, spatial beam profiles of arbitrary complexity may be used in place of the present family of supergaussian.

Optimization studies were made using f/1.5 lenses in each of the 8, 12 and 20 beam configurations. Generally, the best uniformity was obtained for a cubic exponential having a width parameter $a \simeq 0.70$. While the maximum uniformity was found to be comparable for 12 or 20 beams, the 12 beam case seemed vulnerable to misalignment. Eight beam illumination was always found to run a poor third. Typical angles of incidence were $\Psi_{max} \simeq 32^{o}$, indicating considerable loss of energy through refraction. However, by averaging over the angles of incidence and the spatial beam profile, the net refractive loss due to oblique incidence was found to be negligible. In an attempt to reduce this loss, we have also computed 12 beam illumination with

f/1.14 lenses, which take up the same total solid angle as 20 f/1.5 lenses. The result is shown as the plotted circles in Fig. 15. Best uniformity is obtained near $\theta_{max} = 50^{o}$, where $\Psi_{max} \simeq 25^{o}$, reducing refraction losses somewhat. Optimization studies using aplanatic lenses[12] show negligible differences from the above results.

The equality of the coverage angles, θ_m^*, for the dodecahedron and icosahedron is probably due to their close geometrical relationship. (Mathematically they are reciprocals[10] and share the same group properties). Similarly, it may be shown that the coverage angle for the cube is identical to that of its reciprocal, the octahedron. The tetrahedron, on the other hand, is self-reciprocal and has a coverage angle $\theta_m^* = 70.53^{o}$. Thus, we would anticipate much better uniformity for 6 beams ($\theta_m^* = 54.7^{o}$) than for 4 beams, but only slight improvement in going from 6 to 8 beams.

Acknowledgement

I would like to thank R. W. Conn for useful discussions, and E. Anderson and M. Shuy for programming assistance. This research was supported by the Electric Power Research Institute.

References

1. J. Nuckolls, L. Wood, A. Thiessan and G. Zimmerman, Nature 239, 139 (1972). K. A. Brueckner and S. Jorna, Rev. Mod. Phys. 46, 325 (1974).

2. R. E. Kidder, Nucl. Fusion 16, 3 (1976). S. E. Bodner, Phys. Rev. Lett. 33, 761 (1974). J. D. Lindl and W. C. Mead, Phys. Rev. Lett. 34, 1273 (1975).

3. G. H. McCall and R. L. Morse, Laser Focus, Dec. 1974, p. 40. J. F. Holzrichter et al., Bull. Am. Phys. Soc. 20, 1266 (1975).

4. N. G. Basov et al., Lebedev Institute Preprint No. 74, Moscow (1976).

5. Lawrence Livermore Laboratory Laser Program Annual Report (1974), UCRL-50021-74.

6. C. E. Thomas, Appl. Optics 14, 1267 (1974).

7. J. E. Howard, Univ. of Wisconsin Nuclear Engineering Dept. Report UWFDM-188, 1977.

8. Univ. of Wisconsin Nuclear Engineering Dept. Report UWFDM-191, Section III-B, 1977.

9. Laser Focus, May 1976, p. 48.

10. H. S. M. Coxeter, Introduction to Geometry, 2nd ed., Wiley (New York) 1969, p. 152.

11. F. Klein, Lectures on the Icosahedron, Dover (N.Y.), 1956.

12. W. A. Kleinhaus, Appl. Optics 15, 14 (1976).

13. Lawrence Livermore Laboratory Laser Program Annual Report (1974), UCRL-50021-74, p. 135.

14. Ibid., p. 169.

15. Ibid., p. 200.

16. J. P. Freidberg, R. W. Mitchell, R. L. Morse and L. I. Rudsinski, Phys. Rev. Lett. 28, 795 (1972).

17. K. G. Estabrook, E. J. Valeo and W. L. Kruer, Phys. Fluids 18, 1151 (1975).

Figure Captions

Fig. 1. The Platonic solids.

Fig. 2. Definition of the dihedral angle α and wedge angle β.

Fig. 3. Target illumination geometry for an ideal lens (not to scale).

Fig. 4. Beam overlap geometry for icosahedron, showing the fundamental region OAA'. Spherical polar coordinates are chosen with axis coincident with the optical axis of beam 0. Note that with arcs OA and OA' equal, the arc AA' is not part of a great circle. The true minimal region is somewhat smaller, with AA' replaced by a portion of a great circle.

Fig. 5. Schlegel diagram for octahedron.

Fig. 6. Schlegel diagram for dodecahedron.

Fig. 7. Schlegel diagram for icosahedron. Only the inner 9 beams contribute for $\theta_{max} \lesssim 70^{0}$.

Fig. 8. Coverage geometry for octahedron.

Fig. 9. Coverage geometry for dodecahedron.

Fig. 10. Coverage geometry for icosahedron.

Fig. 11. Uniformity versus beam overlap angle using Gaussian beams on f/1.5 lenses, width parameter a = 0.50.

Fig. 12. Uniformity versus beam overlap angle using Gaussian beams on f/1.5 lenses, width parameter a = 1.0.

Fig. 13. Uniformity versus beam overlap angle using Gaussian beams on f/1.5 lenses, optimal width parameter a = 0.70.

Fig. 14. Optimized uniformity, using cubic exponential beams on f/1.5 lenses, a = 0.70. Circles are for 12 f/1.14 lenses with a = 0.65, taking up the same total solid angle as 20 f/1.5 lenses. This gives comparable uniformity with smaller angles of incidence.

Fig. 15. Gaussian beam profiles. The case a = 0.70 yields best uniformity.

Fig. 16. Cubic exponential beam profiles. The case a = 0.70, p = 3 yields best uniformity among all supergaussian profiles.

Fig. 17. Maximum angle of incidence versus beam overlap. Smaller angles of incidence give stronger laser absorption.

Fig. 18. Optimized uniformity with total solid angle fraction limited to 10%, suitable for a laser fusion reactor. Again p = 3 and a = 0.70.

Fig. 19. Optimized uniformity with total solid angle fraction limited to 20%. Again p = 3 and a = 0.70.

Figure 1

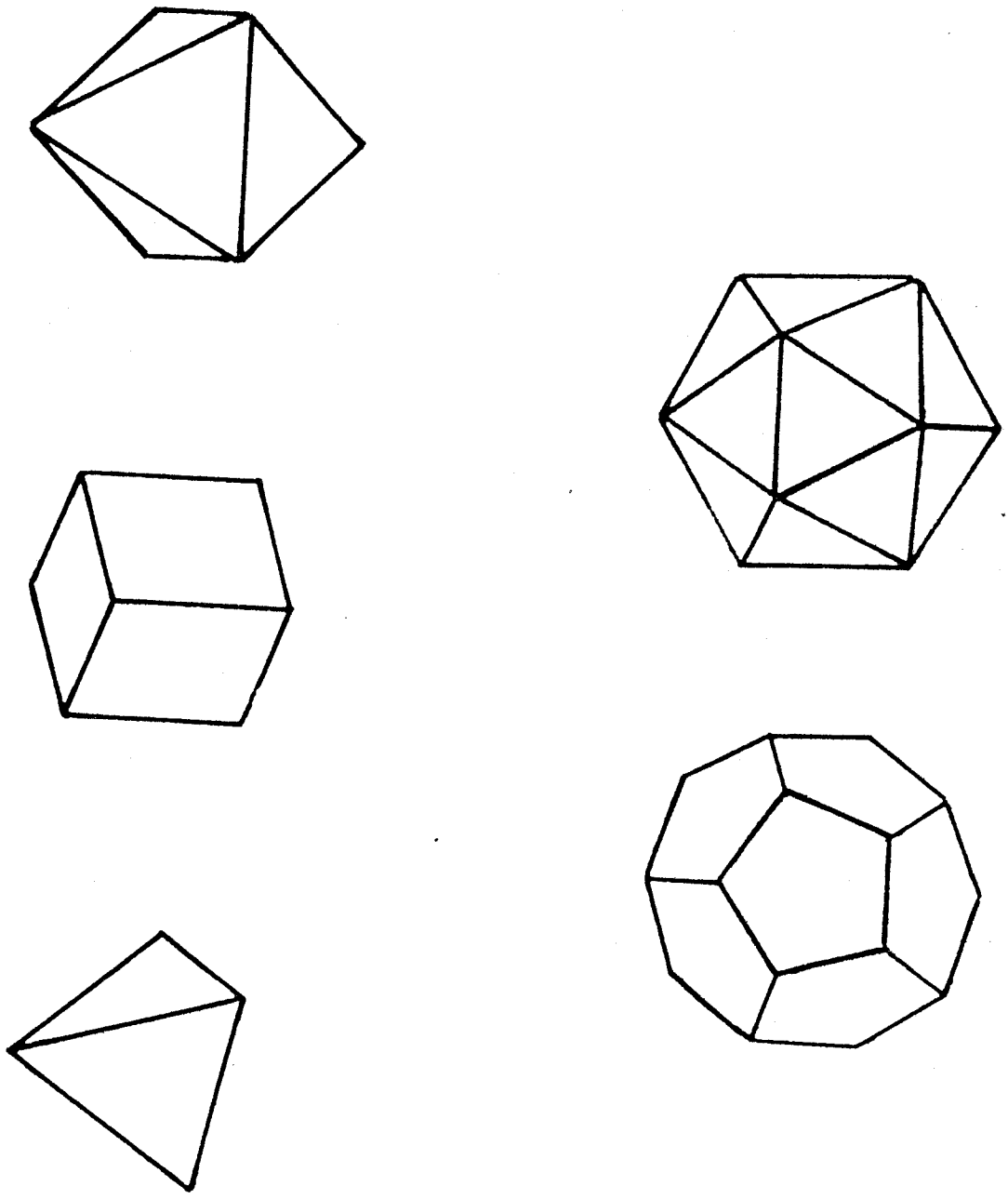

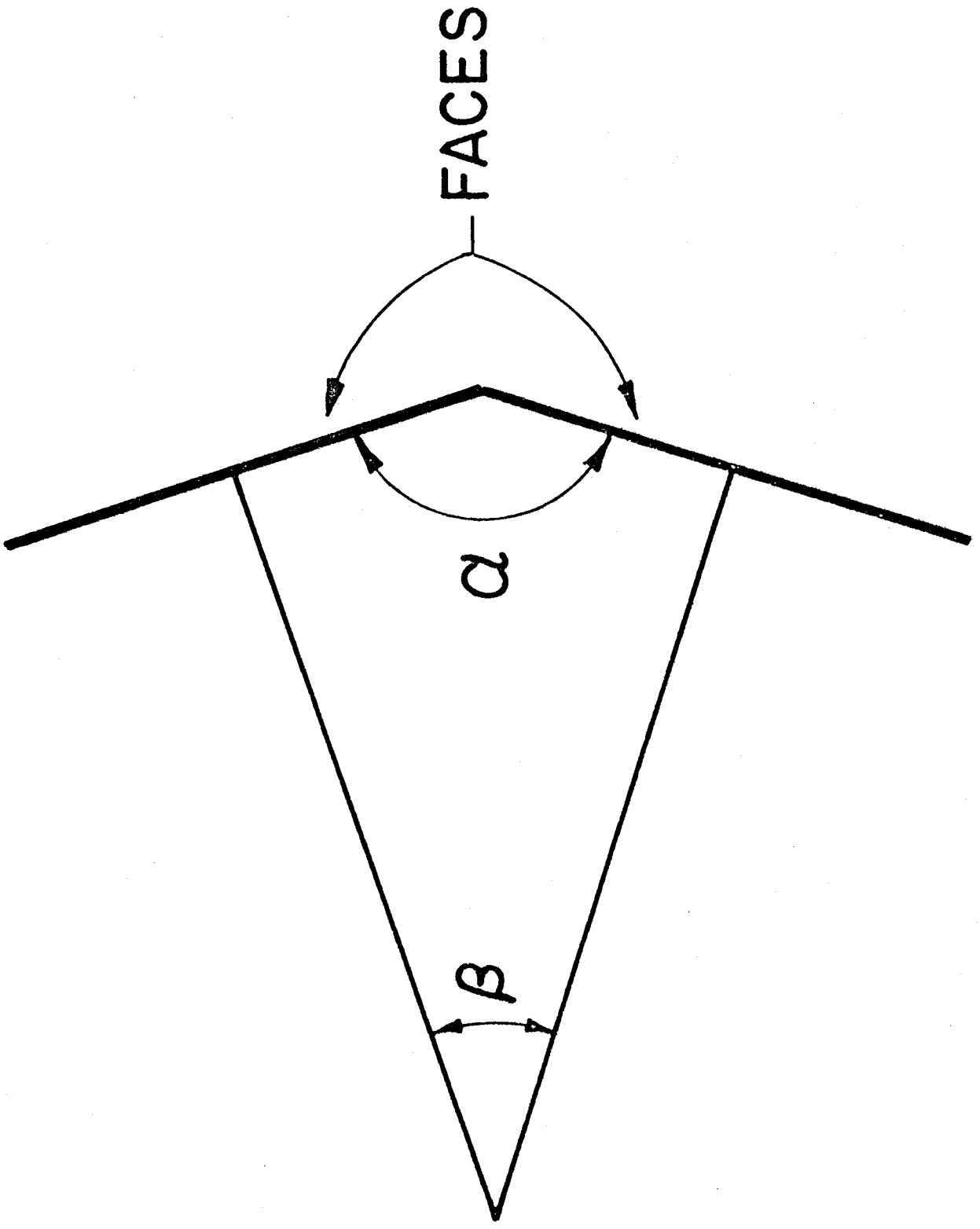

Figure 2

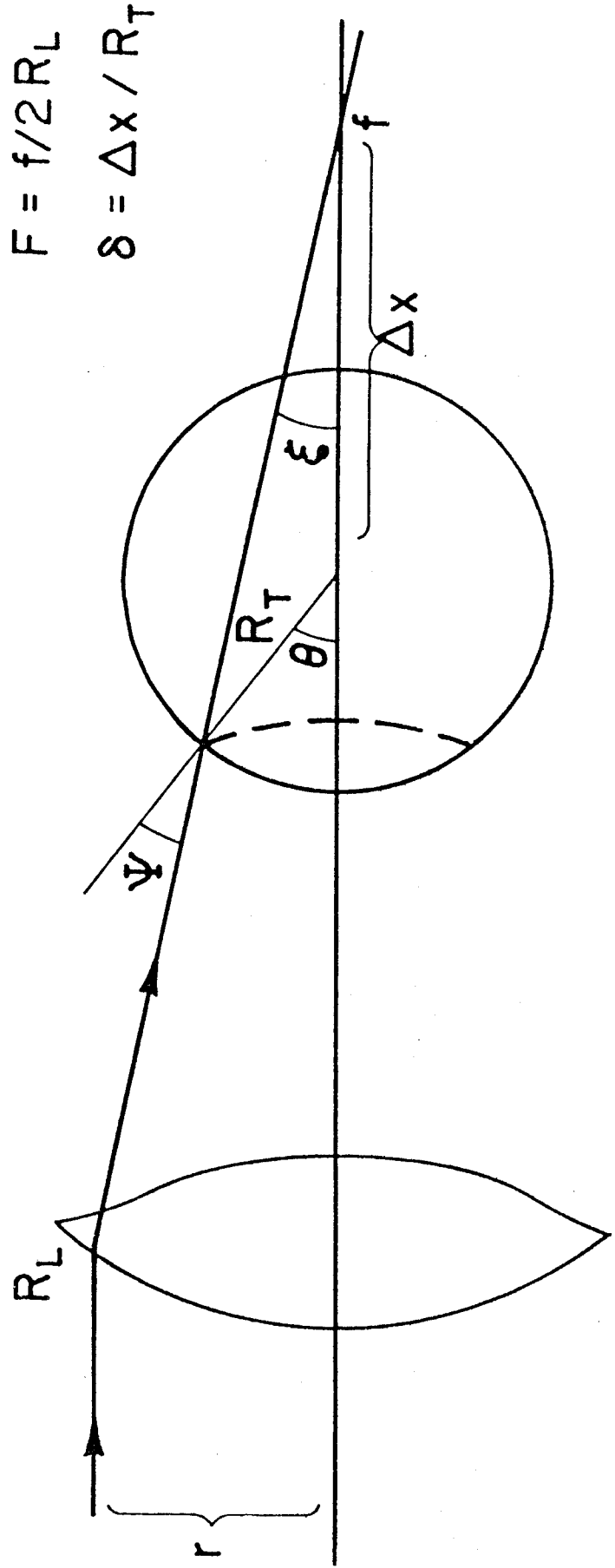

Figure 3

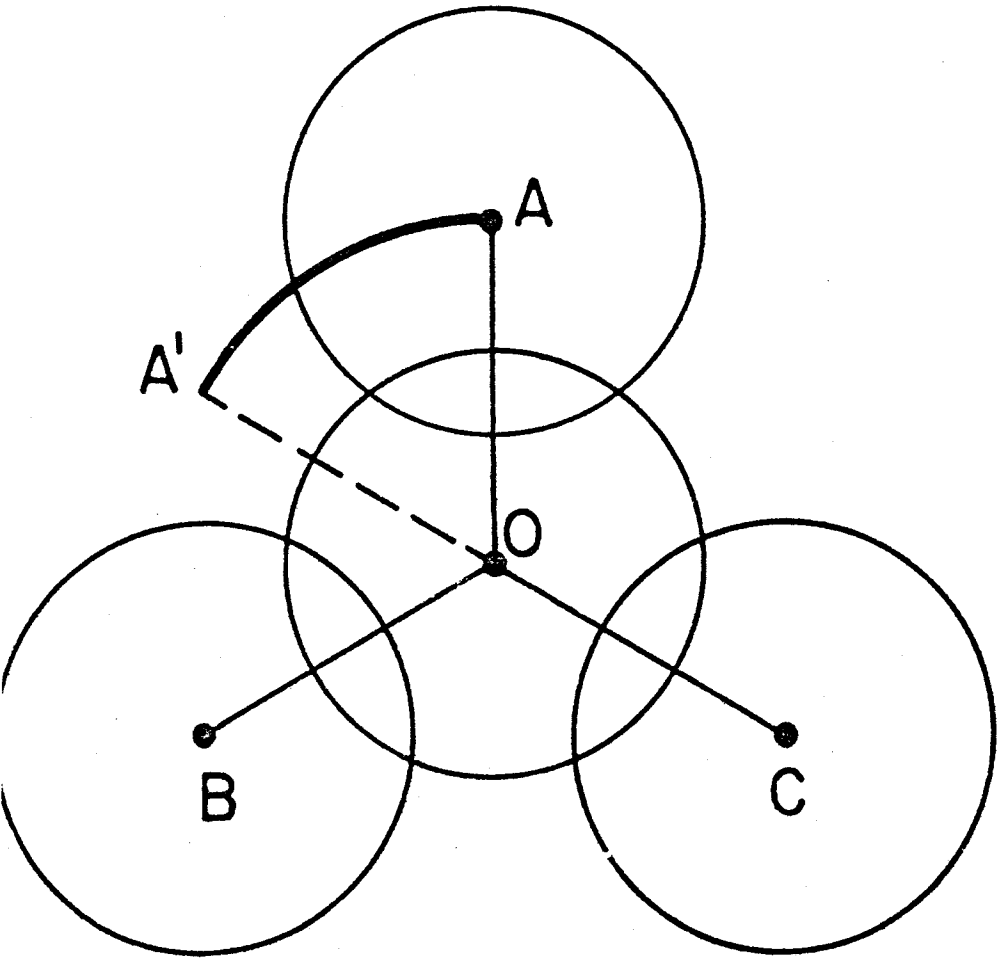

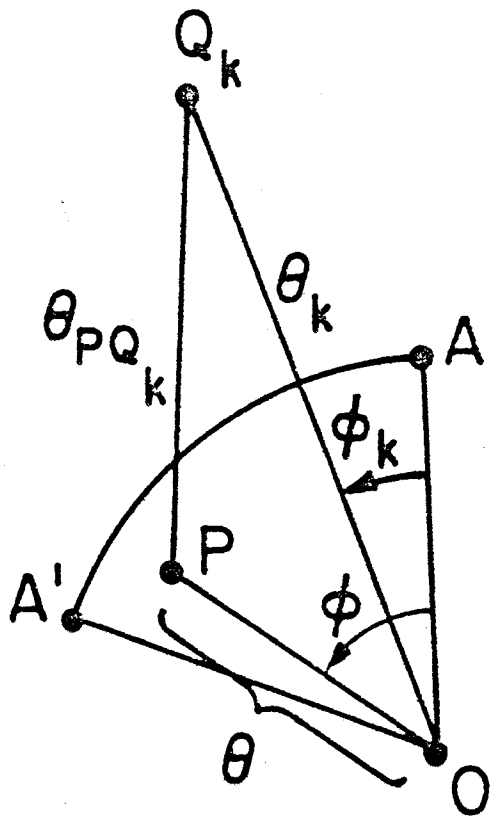

Figure 4

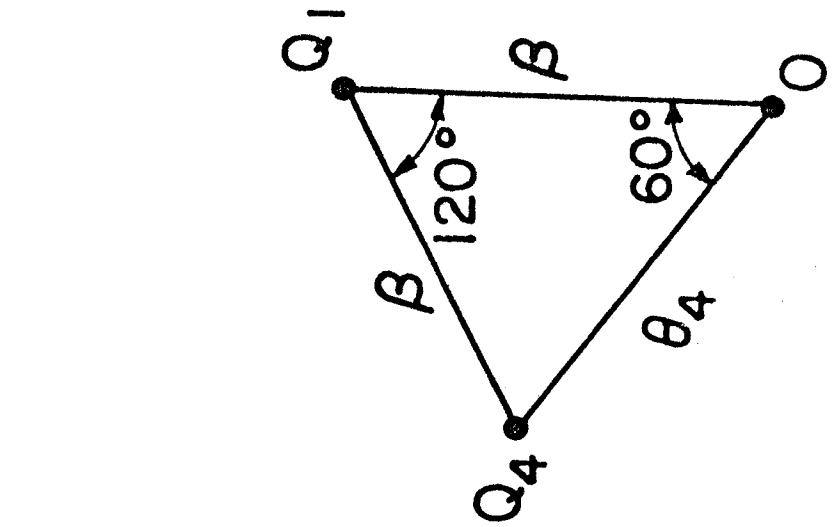

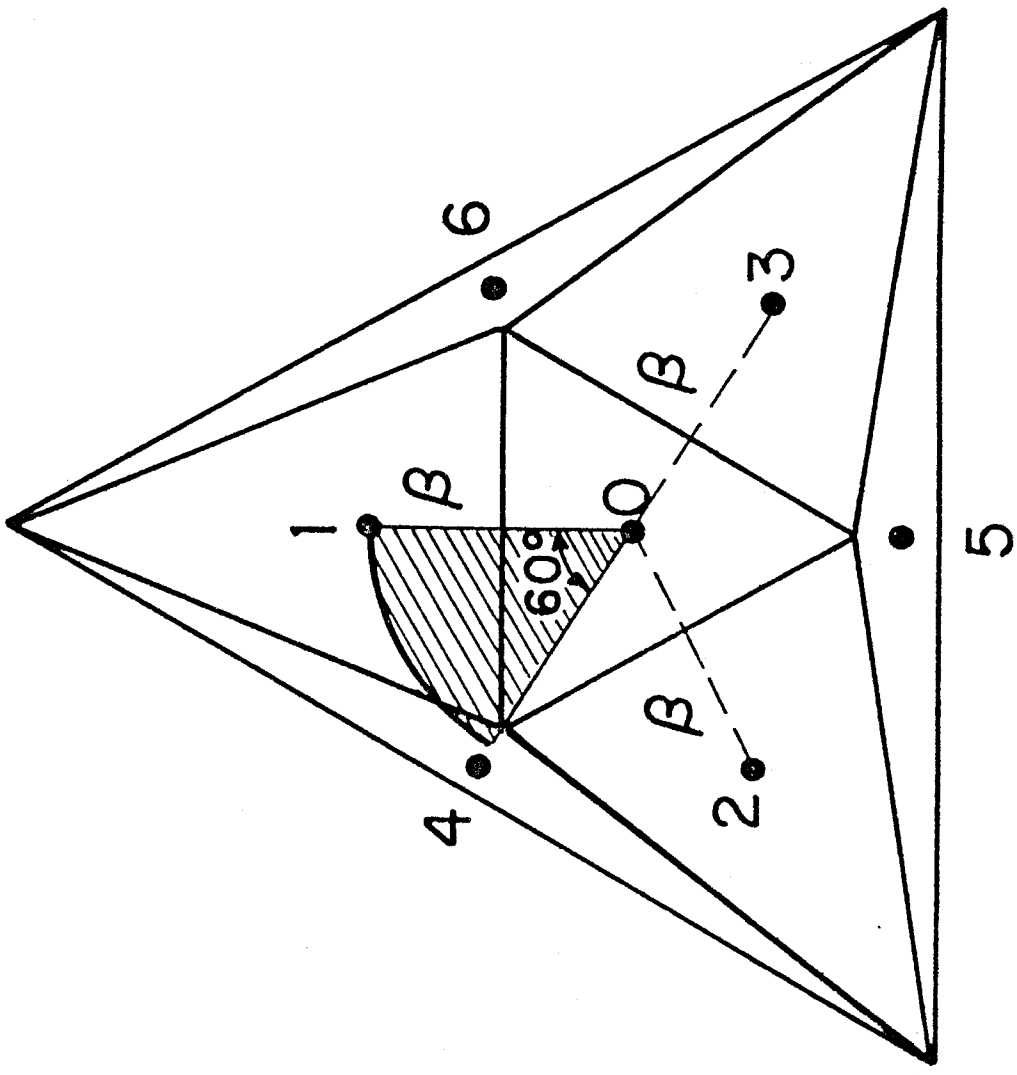

Figure 5

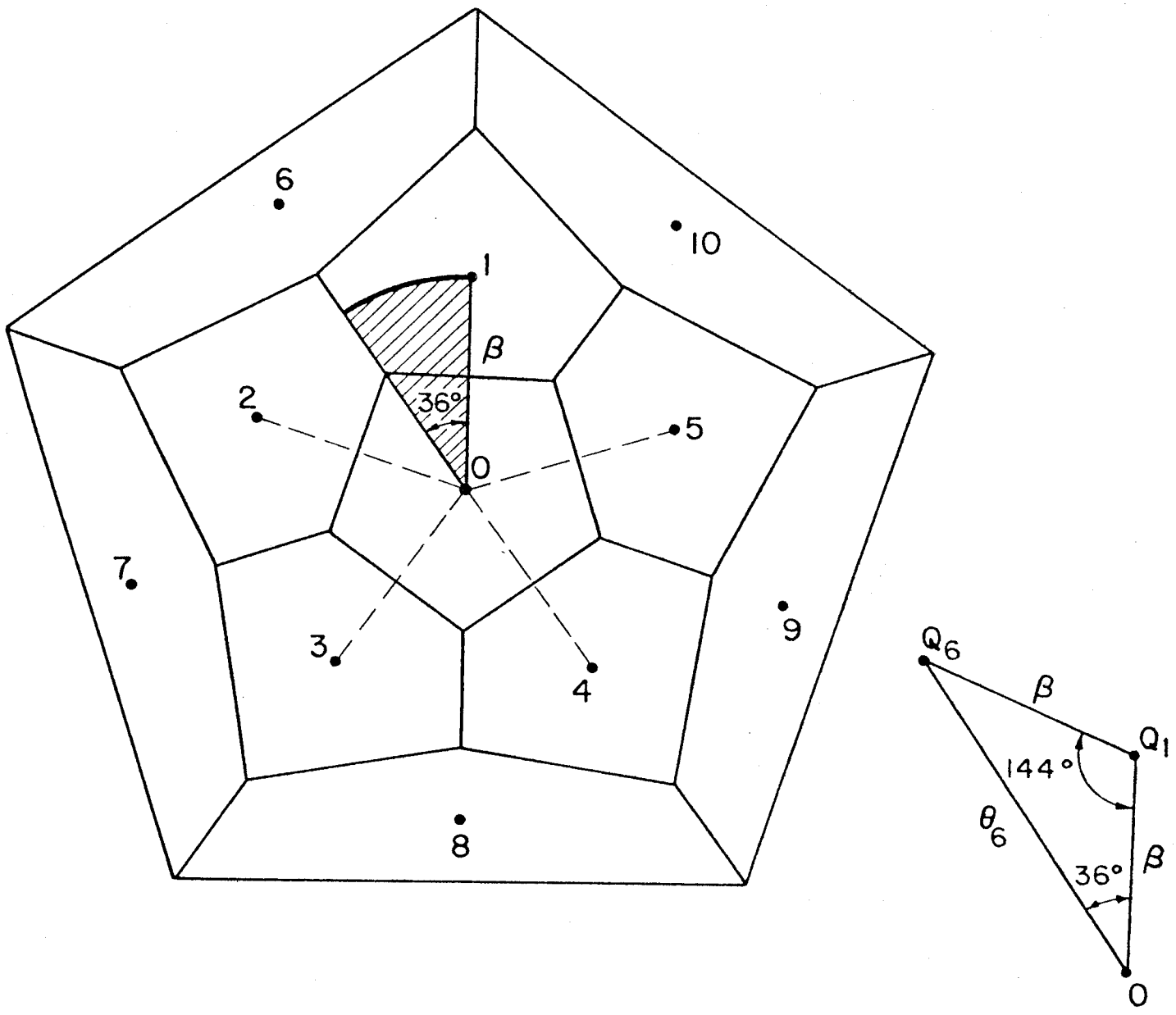

Figure 6

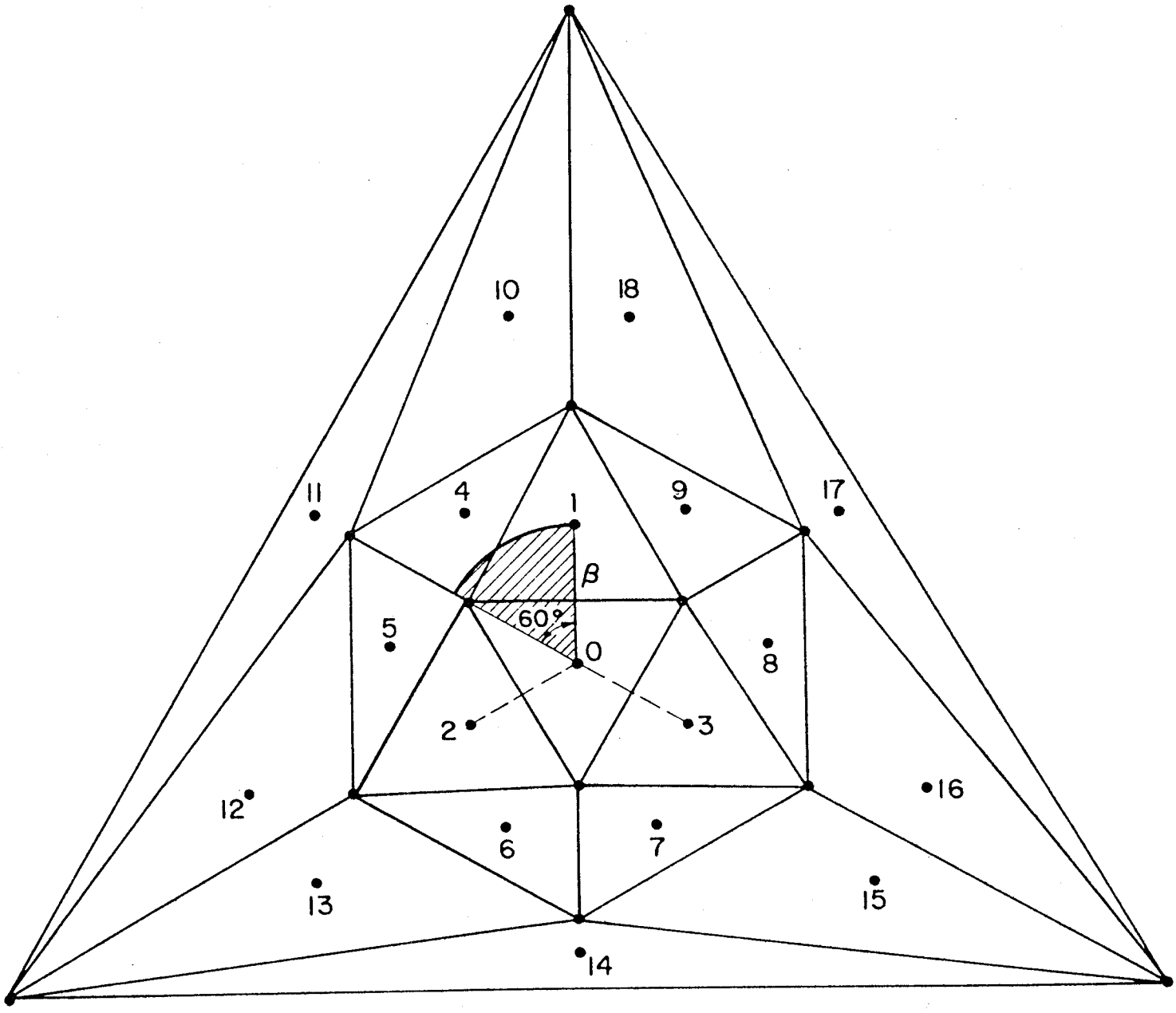

Figure 7

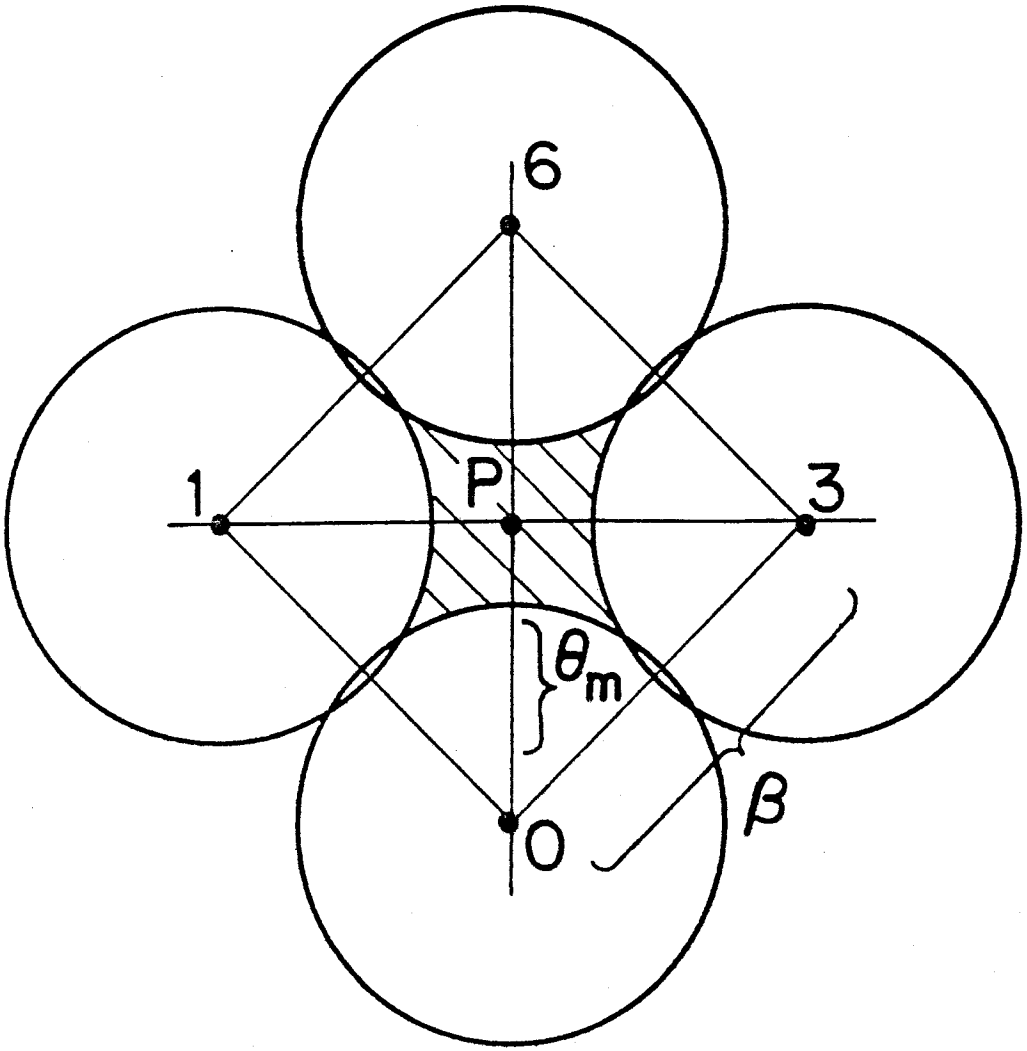

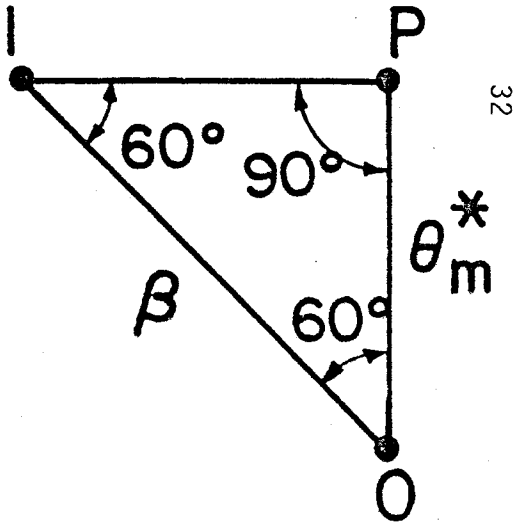

Figure 8

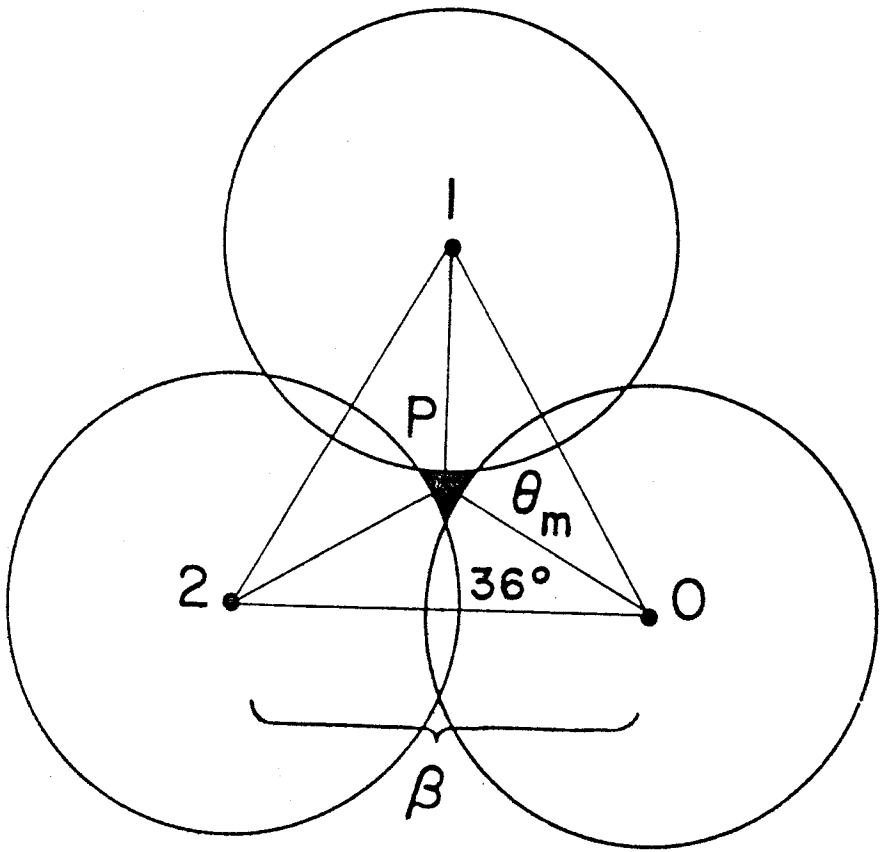

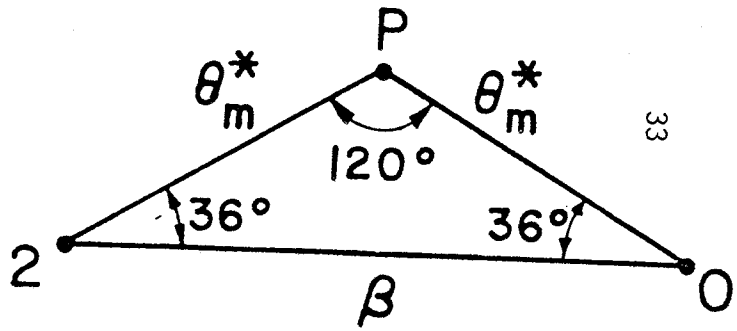

Figure 9

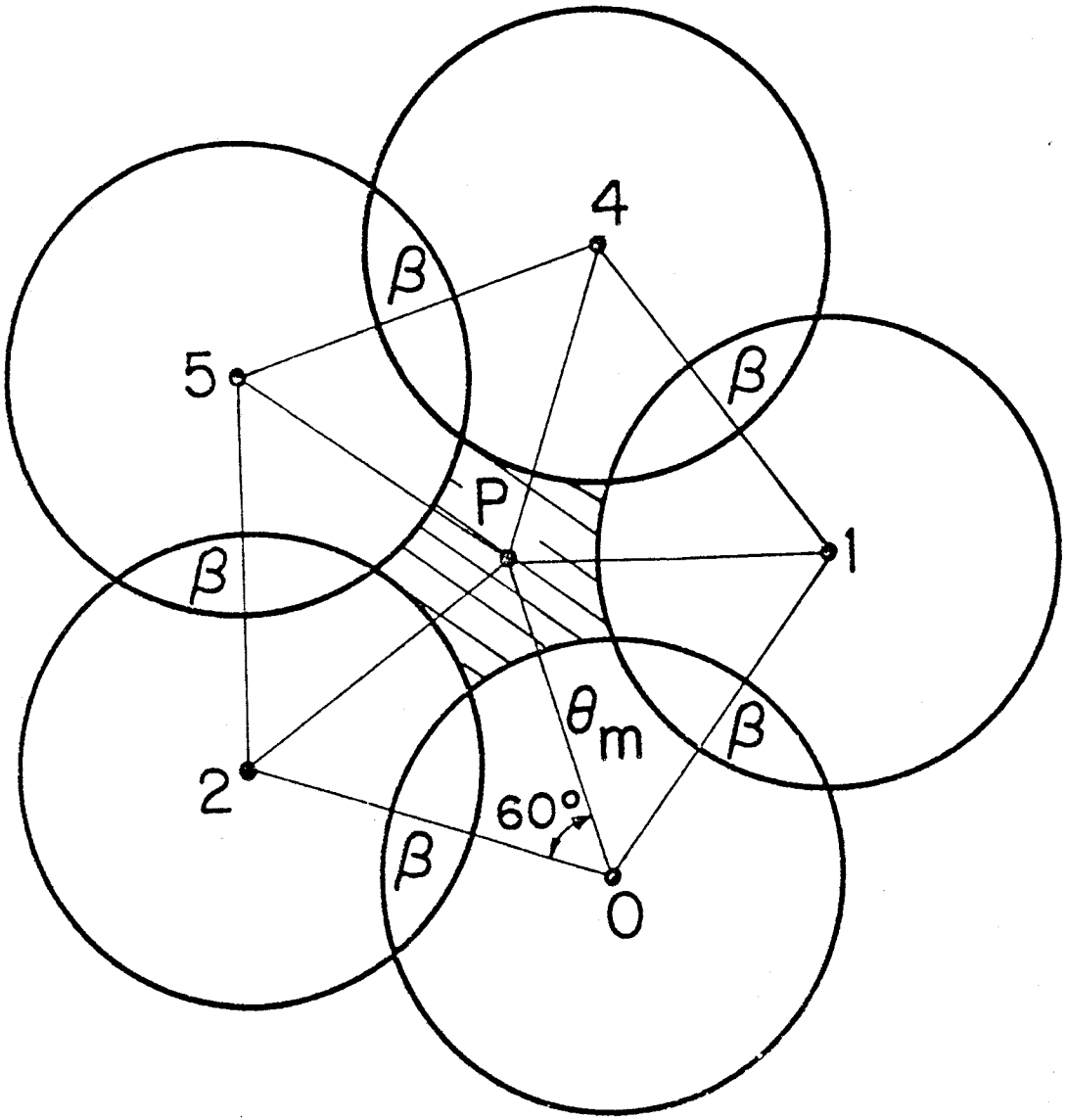

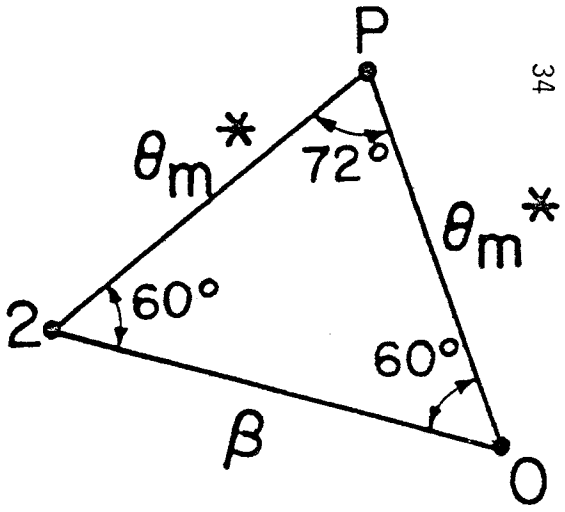

Figure 10

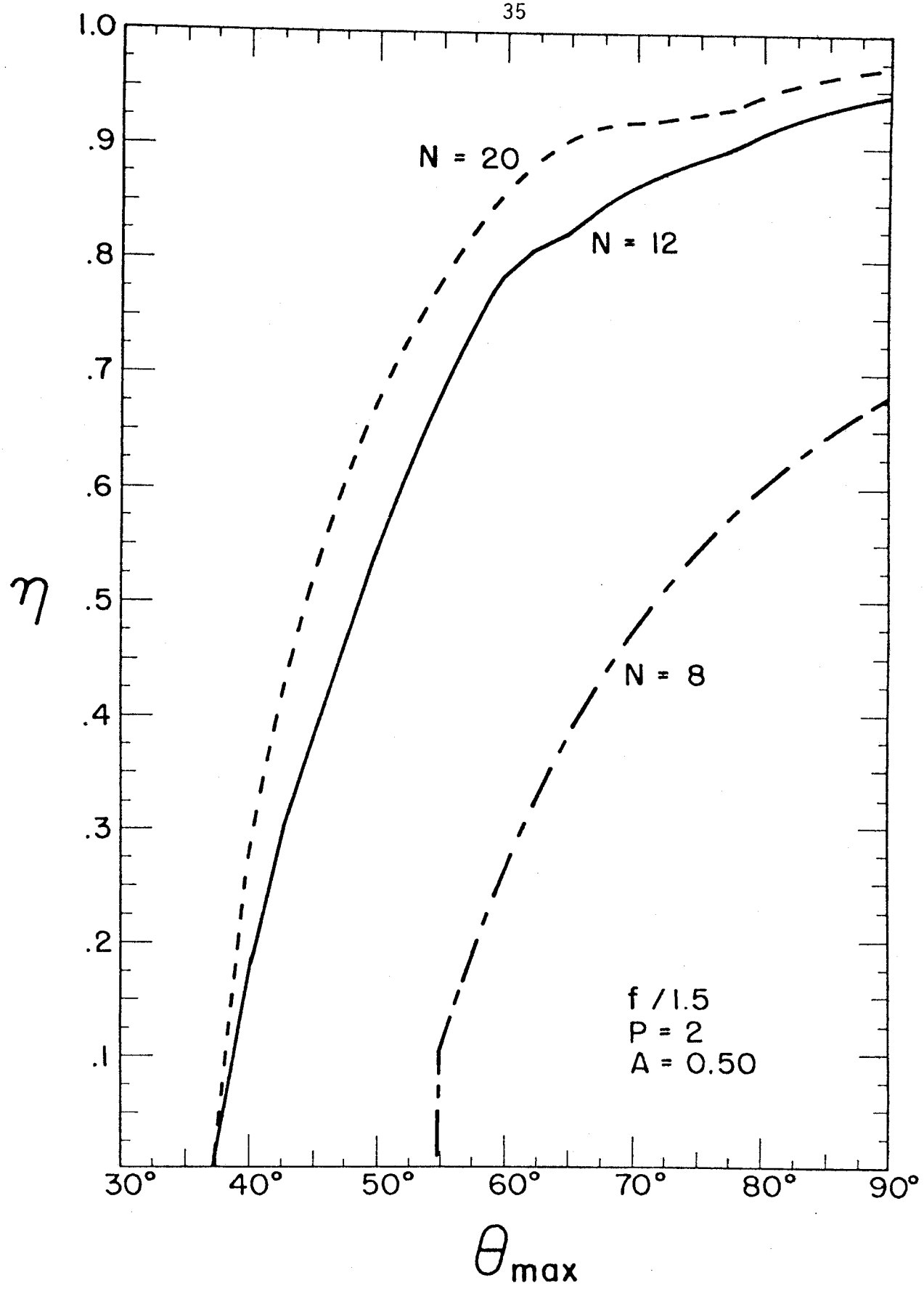

Figure 11

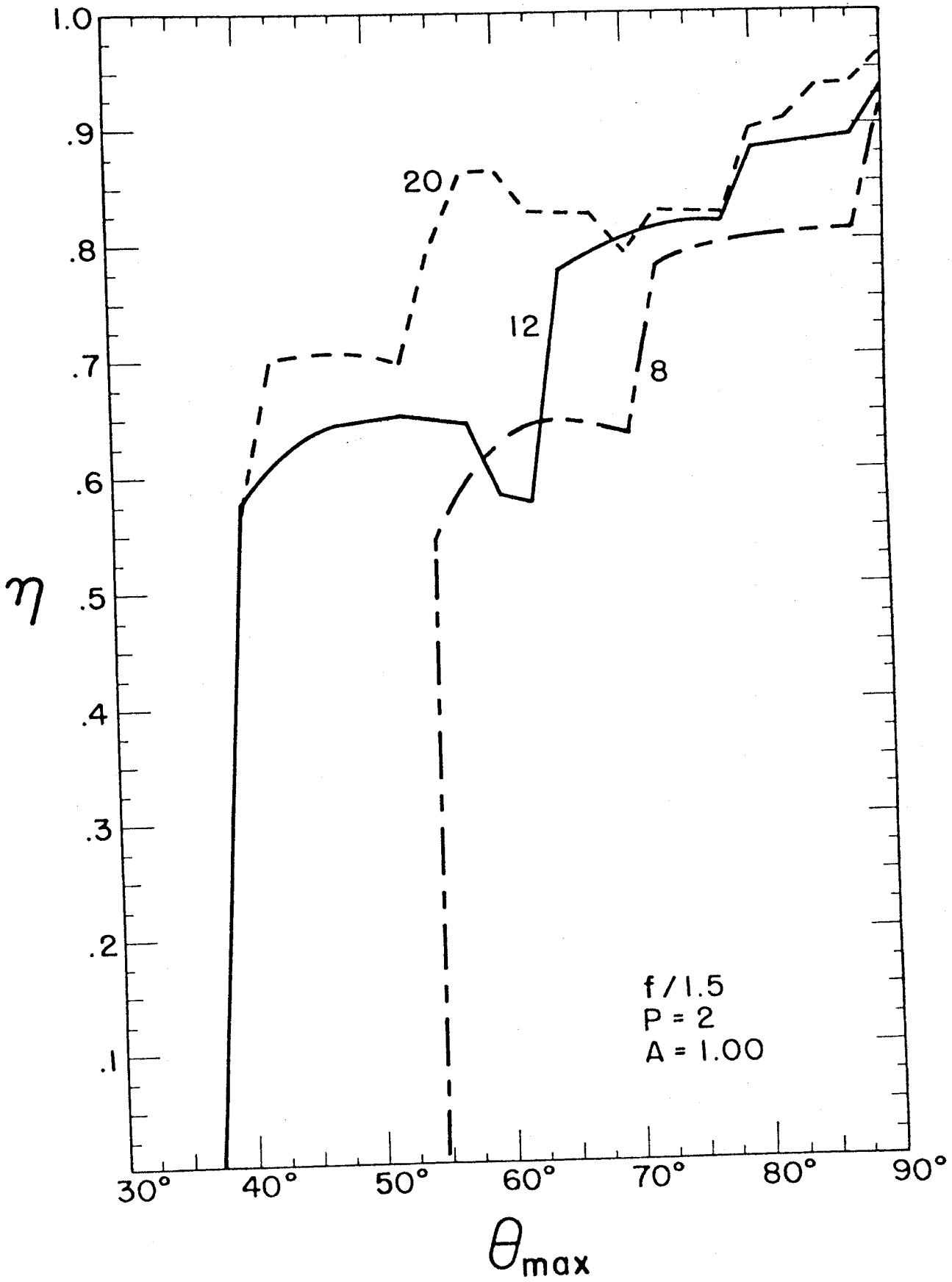

Figure 12

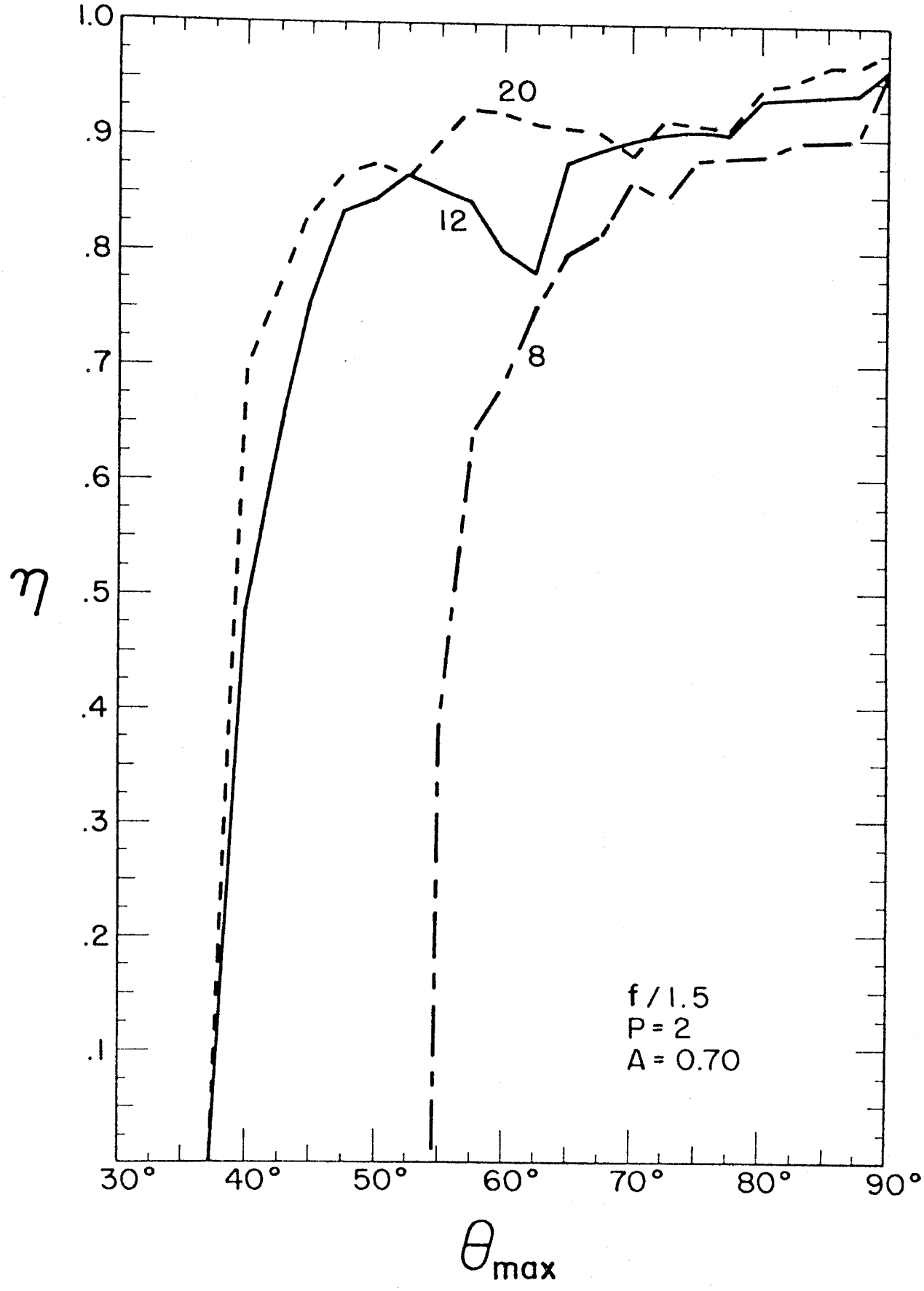

Figure 13

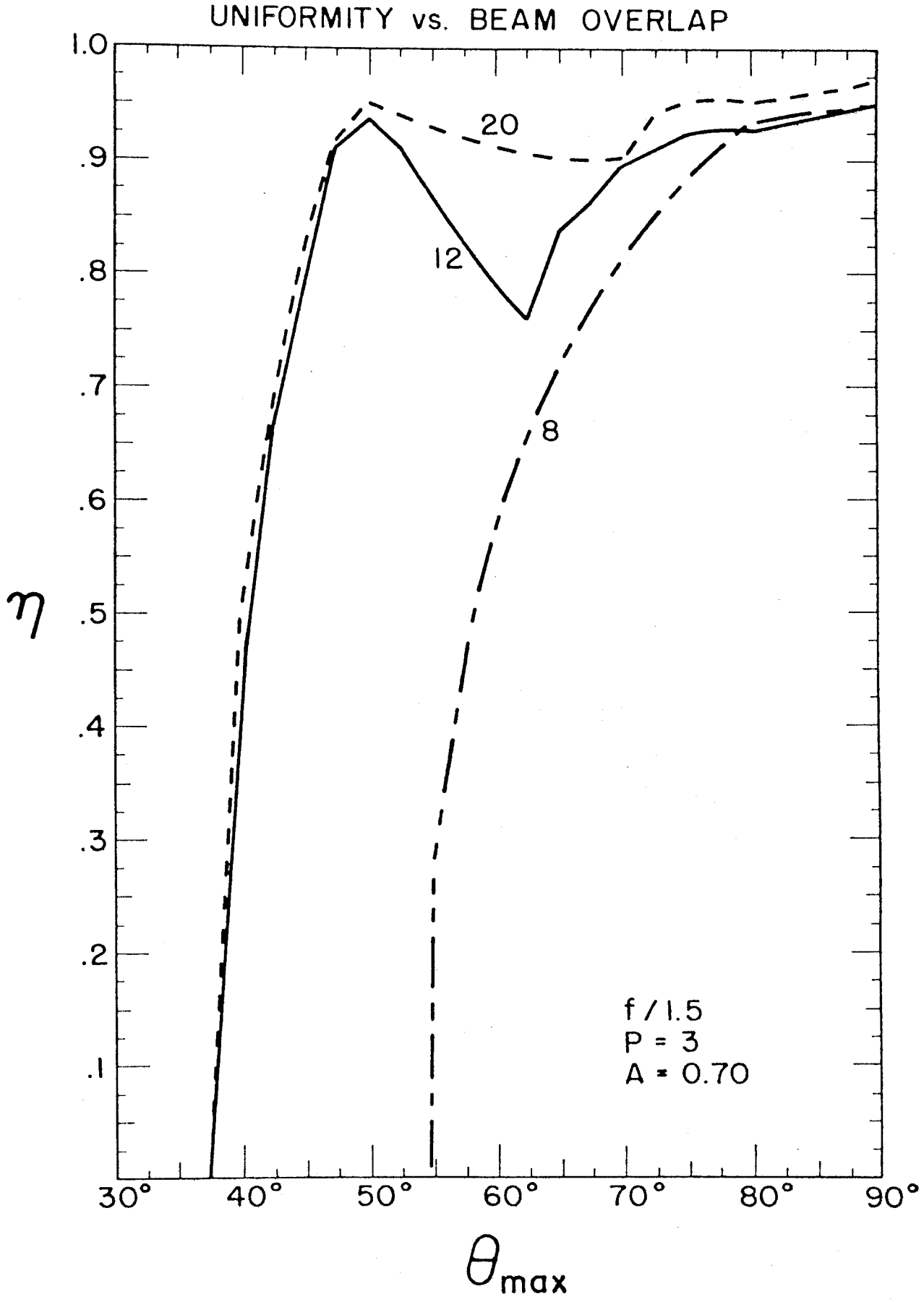
UNIFORMITY vs. BEAM OVERLAP
1.0
.9
.8
.7
.6
.5
.4
.3
.2
.1
η
20
12
8
f / 1.5
P = 3
A = 0.70
30°
40°
50°
60°
70°
80°
90°
θmax

Figure 14

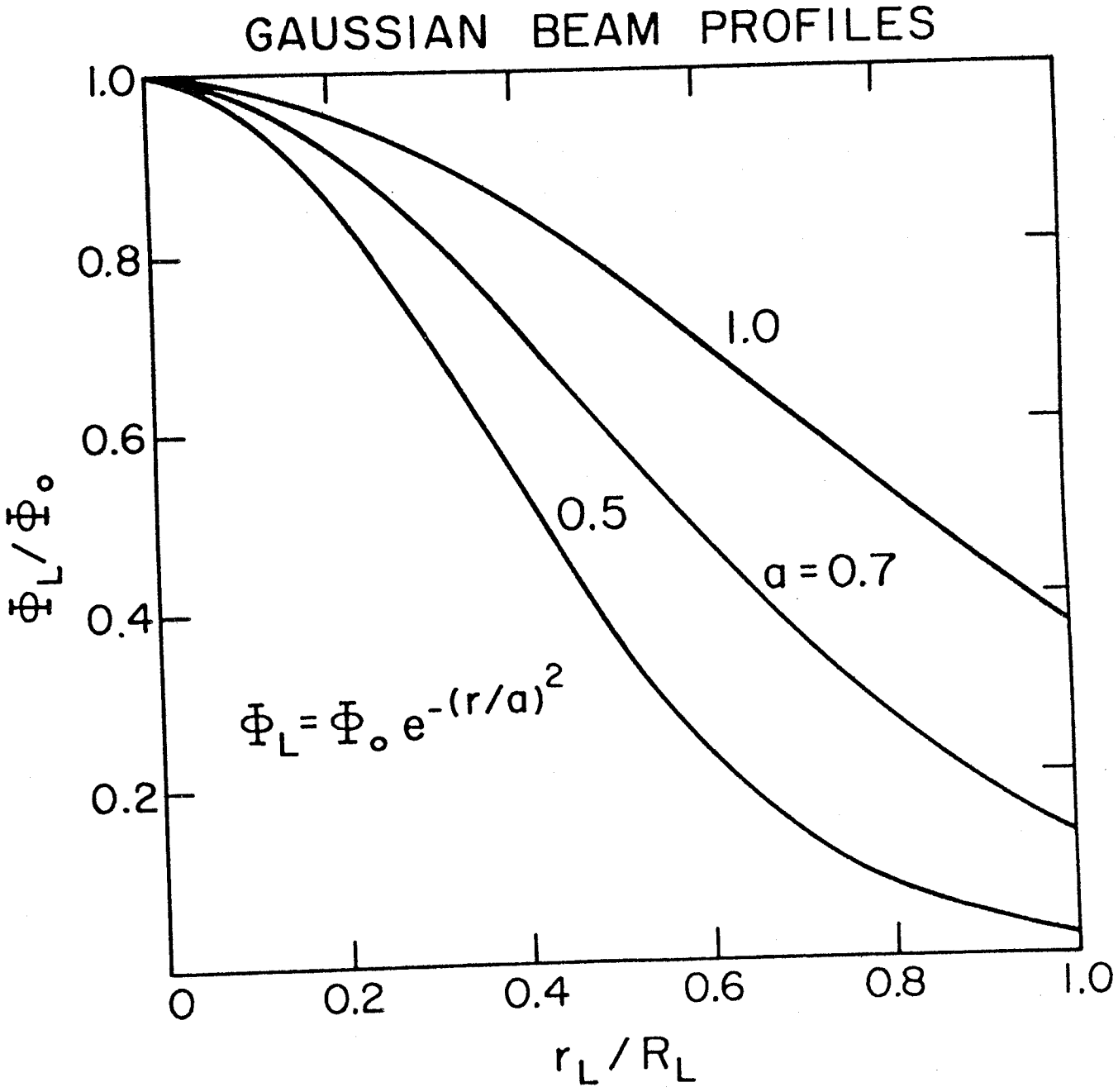
GAUSSIAN BEAM PROFILES
1.0
0.8
0.6
0.4
0.2
0
0.2
0.4
0.6
0.8
1.0
Φ_L / Φ_o
r_L / R_L
1.0
0.5
a = 0.7
$\Phi_L = \Phi_o e^{-(r/a)^2}$

Figure 15

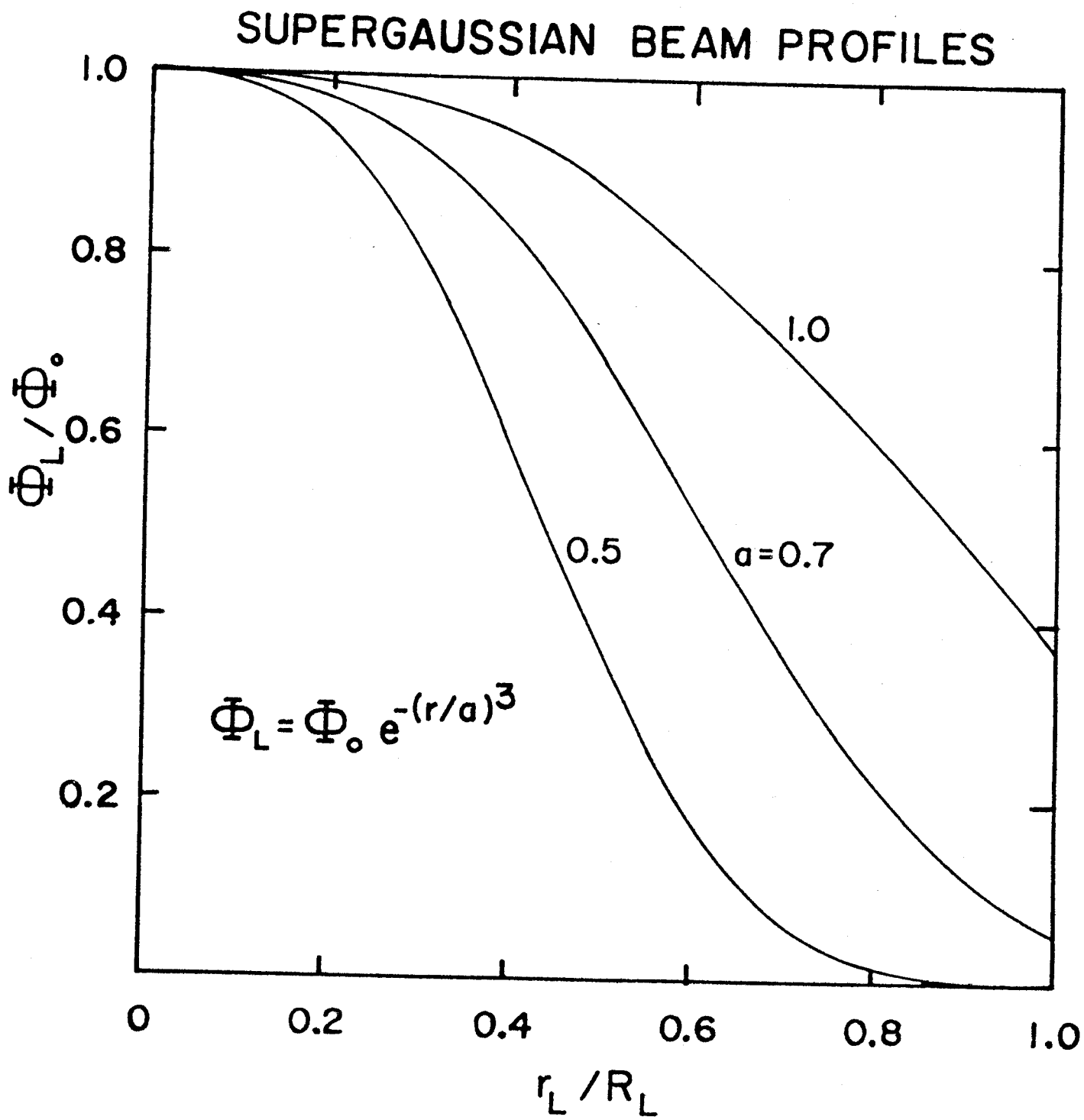
SUPERGAUSSIAN BEAM PROFILES
1.0
0.8
0.6
0.4
0.2
0
0.2
0.4
0.6
0.8
1.0
Φ_L / Φ_o
r_L / R_L
1.0
0.5
a=0.7
$\Phi_L = \Phi_o e^{-(r/a)^3}$

Figure 16

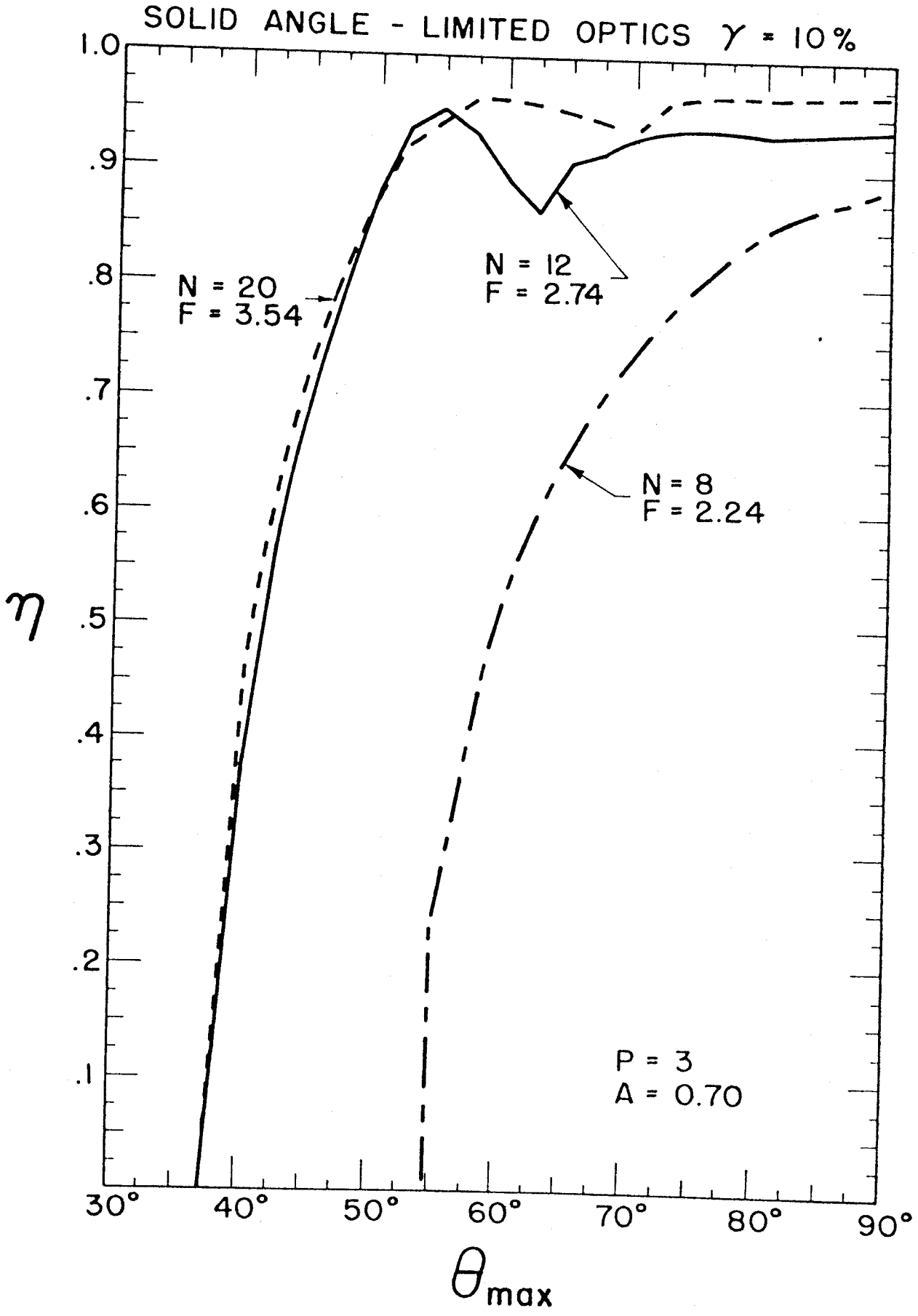
SOLID ANGLE - LIMITED OPTICS γ = 10%
1.0
.9
.8
.7
.6
.5
.4
.3
.2
.1
η
N = 20
F = 3.54
N = 12
F = 2.74
N = 8
F = 2.24
P = 3
A = 0.70
30°
40°
50°
60°
70°
80°
90°
θmax

Figure 18

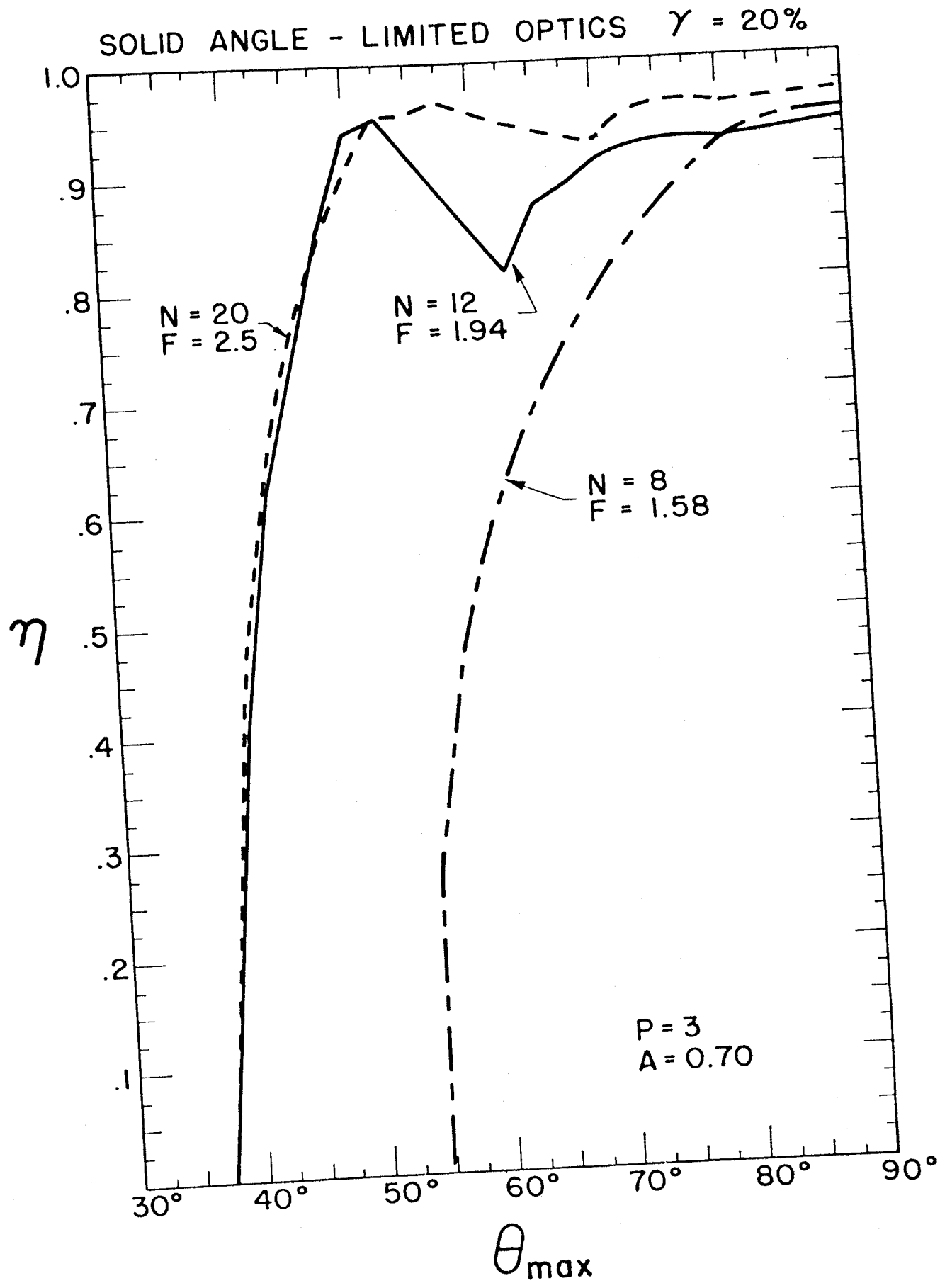
SOLID ANGLE - LIMITED OPTICS γ = 20%
1.0
.9
.8
.7
.6
.5
.4
.3
.2
.1
η
N = 20
F = 2.5
N = 12
F = 1.94
N = 8
F = 1.58
P = 3
A = 0.70
30°
40°
50°
60°
70°
80°
90°
θmax

Figure 19

	N_S	N_E	N_V	p	q	α	β
Tetrahedron	4	6	4	3	3	70.53	109.47^o
Hexahedron	6	12	8	4	3	90^o	90^o
Octahedron	8	12	6	3	4	109.47^o	70.53^o
Dodecahedron	12	30	20	5	3	116.57^o	63.43^o
Icosahedron	20	30	12	3	5	138.18^o	41.82^o

Table 1. Properties of the Platonic Solids

N	$\gamma = 0.1$	$\gamma = 0.2$
4	1.58	1.12
8	2.24	1.58
12	2.74	1.94
20	3.54	2.50

Table 2. Minimum f/nos. for Specified Maximum Solid Angle Taken up by Beams

p \ a	.5	.70	.75	1.0
2	.2454	.4263	.4674	.6321
3	.2257	.4310	.4841	.6998
4	.2216	.4326	.4926	.7468
5	.2218	.4346	.4978	.7813

Table 3. Fill Factors for Supergaussian Beam Profiles